

In Situ Measurements of Temperature in a Coal-Fired Power Plant Using Tunable Diode Laser Absorption Spectroscopy

T. P. Jenkinsⁱ, J. L. Bergmansⁱⁱ, P. A. DeBarberⁱ, M.R. Coffeyⁱⁱⁱ, G.M.C. Starnesⁱⁱⁱ

ⁱMetroLaser, Inc., Irvine, CA

ⁱⁱBergmans Mechatronics LLC, Madison, AL

ⁱⁱⁱEPRI Instrumentation & Control Center, Harriman, TN

AFRC/JFRC 2004 Joint International Symposium, Maui, October 10 – 13, 2004

Abstract:

A new non-intrusive *in situ* temperature sensor has been developed primarily for combustion gas measurement and process control applications that offers high accuracy, large dynamic range, affordability, ruggedness, and high temporal resolution. This achievement was made possible by combining low-cost telecom components with efficient data collection and spectroscopic measurement strategies. The measurement technique is based on line-of-sight infrared absorption spectroscopy. Using fiber optics to couple the sensor to the probe region offers additional flexibility and utility. There are none of the time lag, maintenance, and lifetime problems associated with conventional intrusive probes. The sensor is very well suited to any process in which H₂O is present requiring real-time, non-intrusive temperature sensing, including most industries that rely on combustion, such as automotive, aerospace, aluminum, steel, glass, petroleum, chemicals, forest products, cement, and power generation. Here we present results from measurements in a coal-fired power plant. The data demonstrate the capability of the sensor to make accurate, useful temperature measurements in a harsh industrial environment.

1. Introduction

Absorption spectroscopy using diode lasers has been used for measuring gas temperature and concentration for at least 25 years^{1,2}. However, only recently has the technique begun to appear in industrial settings. Because of their high reliability, low cost, and low power consumption, diode lasers are an ideal light source for industrial gas sensors. Fiber optic technology can be exploited to deliver light to measurement locations using components mass-produced for the telecom industry that are compact, rugged, and reliable. There has been an acceleration in the development and implementation of tunable diode laser absorption spectroscopy (TDLAS) sensors during the past several years, with a broad range of combustion applications having been demonstrated that include industrial^{3,4,5,6} and research^{7,8,9} burners. These joint efforts between research groups and industry have resulted in a number of successful TDLAS sensors that have found use in applications that vary as widely as monitoring an industrial coating deposition process to experiments characterizing a rocket engine exhaust.

Coal-fired power plants are an application that may benefit from TDLAS technology. Despite having been in operation for nearly a century, some of the processes that occur in their combustion chambers are still not completely understood. Being able to accurately measure temperatures in the flame zone can be of critical importance for controlling emissions and optimizing combustion efficiency. However, thermocouple probes can experience reliability issues due to thermal stresses, and optical pyrometers tend to suffer

from inaccuracies caused by a large collection angle and high flame opacity. TDLAS does not suffer from any of these limitations. A previous study in applying TDLAS to coal fired power plants has shown promising qualitative results.⁶

This paper reports on quantitative temperature measurements in a coal-fired power plant obtained using a commercially available TDLAS sensor, the MetroLaser LTS-100.

2. Theory

Absorption spectroscopy involves the precise measurement of the attenuation of a beam of light as it passes through a medium. The inherent technical and conceptual simplicity of the method makes it very attractive for many applications requiring non-intrusive sensing. We use a scanned-wavelength technique to obtain fully resolved H₂O lineshapes from which temperature and H₂O mole fraction can be computed. The technique works as follows.

2.1 Spectral Absorbance

A beam of light of wavelength λ passing through an absorbing medium will be attenuated according to the Beer-Lambert relationship,

$$I(\lambda) = I_o(\lambda) \exp(-\alpha_\lambda), \quad (1)$$

in which $I(\lambda)$ is the beam intensity at wavelength λ after propagation through the absorbing medium, $I_o(\lambda)$ is the incident intensity of the beam, and α_λ is the spectral absorbance. The spectral absorbance of a given chemical species is dependent on species concentration, temperature, and pressure. For a single absorption line, i , this can be expressed by

$$\alpha_{\lambda,i} = P X L S_i(T) \phi_i(\lambda - \lambda_0), \quad (2)$$

where P is the static pressure (atm), X is the mole fraction or relative concentration of the probed species (H₂O, in this case), L is the absorption path length (cm), S_i is the temperature-dependent linestrength specific to line i (cm⁻²/atm), and $\phi_i(\lambda - \lambda_0)$ is the lineshape function (cm), which accounts for spectral broadening of the absorption line. The lineshape function is defined such that

$$\int_{-\infty}^{\infty} \phi(\lambda - \lambda_0) d\lambda = 1. \quad (3)$$

Two kinds of broadening are typically dominant in gaseous flows, Doppler broadening and collisional broadening. Doppler broadening is caused by shifts in the resonant wavelengths of the molecules due to their motion relative to the light source. Since the velocities of molecules in a gas are dependent upon temperature, Doppler broadening is a function of temperature. Collisional broadening is caused by reductions in the lifetimes of the energy states of molecules because of collisions with other molecules. According to the Heisenberg uncertainty principle, the uncertainty in the energy of a molecule is inversely related to the uncertainty in the lifetime at that energy level, or

$$\Delta E = \frac{h}{2\pi} \frac{1}{\Delta t}. \quad (4)$$

Thus, the energy transition that corresponds to a particular absorption line will involve some uncertainty in the upper and lower state energies, leading to an uncertainty in the energy difference between them that determines the wavelength of light absorbed. A lineshape with both Doppler and collisional broadening can be accurately modeled using a Voigt function, which is a convolution of a Gaussian and a Lorentzian function, if the temperature and the collisional broadening coefficients are known. The temperature can be obtained by taking a ratio of areas under two different absorption lines, as described next.

2.2 Temperature

The linestrength of a given line changes with temperature according to the Boltzmann populations of the energy states,¹⁰

$$S_i(T) = S_{i,0} \frac{Q_0}{Q(T)} \exp \left[-\frac{hcE_i''}{k} \left(\frac{1}{T} - \frac{1}{T_0} \right) \right] \times \left[\frac{1 - \exp(-hcE_i''/kT)}{1 - \exp(-hcE_i''/kT_0)} \right] \quad (5)$$

where $S_{i,0}$ is the linestrength at a reference temperature T_0 , usually taken to be 73 °F. The linestrength and the lower state energy, E_i'' , are spectroscopic constants that are specific to the absorption line. $Q(T)$ is the total internal energy partition function, specific to the molecule, and Q_0 is it's value at T_0 . The last multiplier, in brackets, accounts for stimulated emission, and is negligible at wavelengths less than 2.5 μm and temperatures below 2500 K. Equation (5) shows that the linestrength is a function of temperature only. In practice, the measured $\alpha_{\lambda,i}$ is related to the linestrength by Eq. (2). By scanning the laser wavelength over the lineshape and summing the measurements of $\alpha_{\lambda,i}$, the lineshape function, $\phi_i(\lambda-\lambda_0)$, integrates to unity, removing any dependence on Doppler or collisional broadening. Integrating both sides of Eq. (2), we have

$$\int_{-\infty}^{\infty} \alpha_{\lambda,i} d\lambda = PXL S_i(T) \quad (6)$$

where $\int_{-\infty}^{\infty} \alpha_{\lambda,i} d\lambda$ is the area under absorption line i . When two absorption lines are scanned simultaneously, the ratio of their areas becomes equal to the ratio of their linestrengths. Using **Eqs. (5) and (6)**, this ratio becomes

$$R = \frac{\int_{-\infty}^{\infty} \alpha_{\lambda,1} d\lambda}{\int_{-\infty}^{\infty} \alpha_{\lambda,2} d\lambda} = \frac{S_{1,0}}{S_{2,0}} \exp \left[-\frac{hc(E_1'' - E_2'')}{k} \left(\frac{1}{T} - \frac{1}{T_0} \right) \right] \quad (7)$$

Note that in Eq. (7) P , X , and L for the two lines cancel. Equation (7) shows that the ratio of areas is a function of temperature only.

In practice, it is difficult to find two isolated H_2O lines in the near-IR, where lasers are readily available, since there are so many lines that they tend to overlap, especially at high temperatures. However, groups of lines can sometimes be found that behave like a

two-line system. For example, Figure 1 shows a simulated spectrum of the H₂O molecule near 1500 nm, based on spectroscopic data from the HITRAN¹¹ database. Two prominent features can be seen that appear as individual lines, although they are each actually made up of multiple lines. Each feature has a different dependence on temperature. In this case, the feature at lower energy increases with temperature and the feature at higher energy decreases with temperature. Figure 2 shows the ratio of areas under these two features as a function of temperature for pressures of 0.5, 1, and 3 atm. Since the ratio increases monotonically with temperature, these features offer a good solution for a temperature diagnostic. The plot also shows that this ratio is very insensitive to pressure. This is the line pair used in the LTS-100 sensor system that was applied to measurements in a coal-fired power plant furnace described later in this paper.

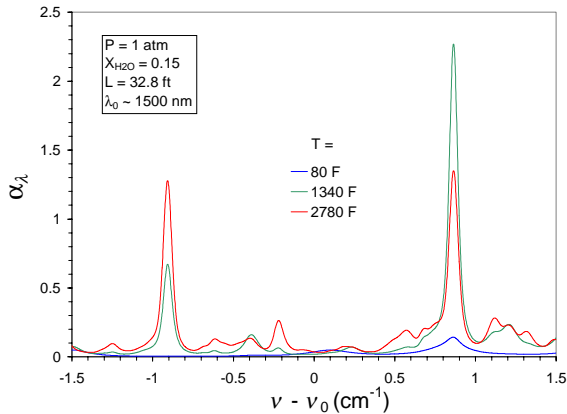


Figure 1. Simulated H₂O absorbance spectrum near 1500 nm showing two features that have different temperature dependence.

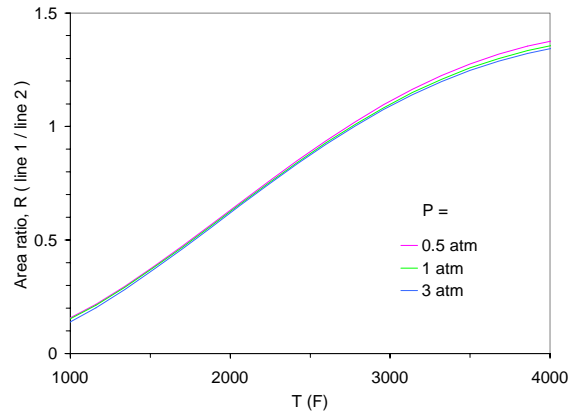


Figure 2. Simulated area ratio of H₂O line pair near 1500 nm.

3. Implementation and Calibration

To implement the technique, the laser wavelength is scanned over the two H₂O lines and the transmitted intensity $I(\lambda)$ is measured. The scan is accomplished using a ramp function to drive the diode laser current. This causes the laser intensity to ramp as well. Figure 3 gives a graphical description of the process. The waveform of the raw signal is depicted on the left side of Figure 3, in which the transmitted intensity, $I(\lambda)$, is ramped with a downward slope. Since the wavelength is also ramping, two dips can be seen corresponding to the absorption lines. The reference intensity, $I_o(\lambda)$, is obtained by curve fitting the baseline portion of the scan, excluding the absorption lines. Using Equation (1), the spectral absorbance, α_λ , is calculated from the transmitted intensity as a function of time, as shown on the right side of Figure 3. Each scan takes approximately 50 μ s, which is a small enough time scale that the thermal conditions can be assumed to be frozen for most applications. Note that the horizontal axis depicted here is time, not wavelength, so the resulting time-domain spectrum is a pseudo spectrum. If an actual wavelength spectrum is desired, it is possible to convert this time axis to wavelength using a wavemeter and a solid etalon to calibrate the tuning characteristics of the laser; alternatively, the known wavelength positions for the selected features may also be used

for absolute wavelength calibration. However, practice has shown that the wavelength vs. time tuning relationship does not vary much from linearity. As described below, the temperature calibration technique used here does not require a conversion of the time axis to wavelength.

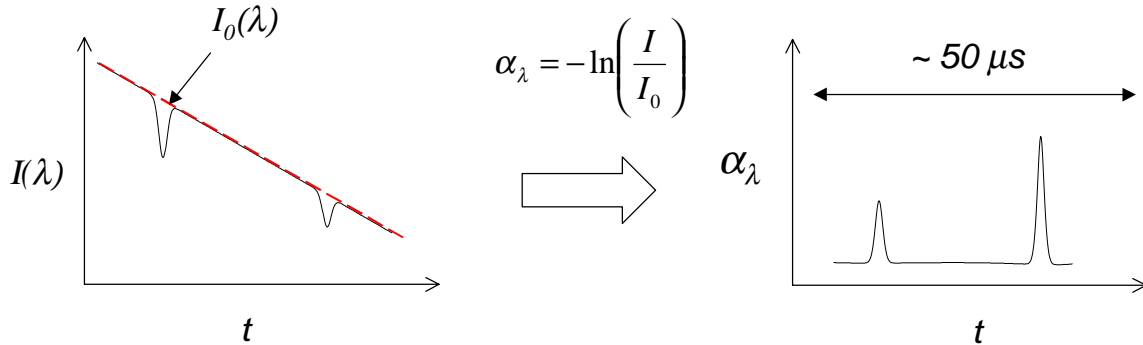


Figure 3. Scanned wavelength technique for measuring spectral absorbance.

Measured absorbance area ratios as a function of temperature may differ somewhat from the theoretical temperature calibration curve shown in Figure 2. Reasons for this include inaccuracies in the spectroscopic database, uncertainty in the calculated baseline absorption, and nonlinearity of the wavelength tuning characteristics of the laser as described above. Therefore, a calibration experiment was conducted to produce a relationship between temperature and area ratio from the time-domain spectrum.

Figure 4 shows the arrangement used for calibration measurements. A flat flame (McKenna) burner was used to produce a premixed one-dimensional flame using either H₂ or natural gas as the fuel, and air as the oxidizer. Switching between the two fuels

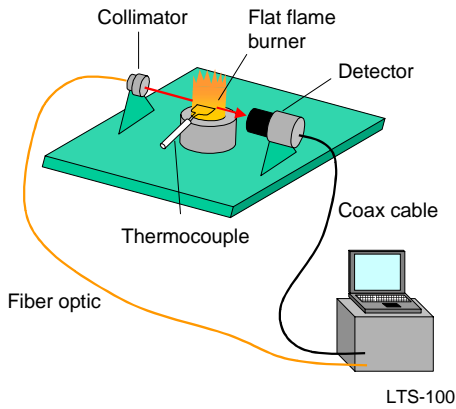


Figure 4. Experimental setup for calibration of the LTS-100 with a thermocouple in a premixed flat flame.

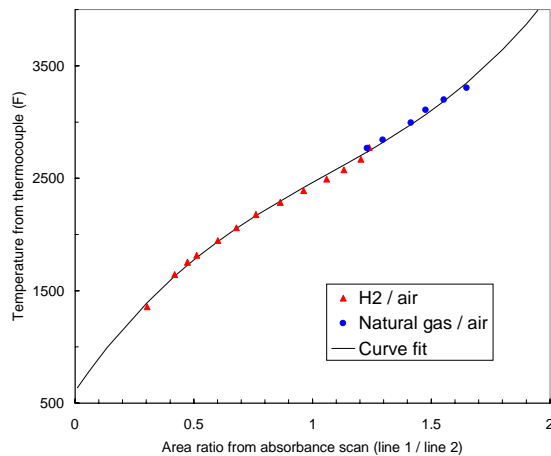


Figure 5. Experimentally obtained calibration curve for the LTS-100 system.

enabled the generation of a range of temperatures from 1300 to 3300 °F. A fine wire S-type thermocouple was used (0.002-in. diameter), with at least 0.5 in. of the leads oriented within the plane of the flame to minimize conduction losses. The beam height was made to coincide with the thermocouple position in a region downstream of the

flame zone, 0.138 in. above the burner surface. At a given equivalence ratio for a given fuel, the indicated thermocouple temperature was stable to within ± 2 °F, and the measured absorbance ratio was stable to within a range corresponding to ± 10 °F. The greater range of the laser-based temperatures results from its 14-ms time response that is able to resolve rapid temperature fluctuations of the flickering flame.

Figure 5 shows the measured temperatures from the thermocouple as a function of absorbance area ratio. Each measurement point represents an average of at least 1000 absorption scans over a time of about 20 seconds, and was corrected for radiations losses to the surroundings. The estimated uncertainty in the thermocouple temperatures is ± 90 °F, due primarily to the uncertainty in the emissivity of the thermocouple bead when making radiation corrections. Using H₂ as the fuel, the highest temperature achievable was about 2750 °F, occurring near stoichiometric conditions. This was considerably less than the theoretical adiabatic flame temperature of 3712 °F. Interestingly, the temperatures using natural gas were higher, even though the theoretical adiabatic flame temperature is lower at 3554 °F. This can be explained by the fact that the H₂ flame was observed to be much closer to the burner surface than the natural gas flame, probably due to the faster kinetics. Thus, the heat loss due to conduction through the unburnt gases to the burner surface would be higher for the H₂ flame, causing a lower equilibrium temperature. The slower kinetics of the natural gas flame prevented combustion from occurring at temperatures below 2745 °F, which was near the maximum temperature of the H₂ flame. When comparing measurements from the H₂ flame with the natural gas flame, a small overlap region of about 10 °F existed around 2750 °F. As Figure 5 shows, the absorbance area ratio agreed between the two flames at this temperature, suggesting that the method is not highly dependent on fuel type. The highest temperatures achievable with the natural gas flame were above 3300 °F, but could not be measured since the thermocouple melted at this temperature. A third order polynomial was fit to the data, shown as the solid line in Figure 5. This polynomial was incorporated into the software of the LTS-100 system to provide real-time temperatures from the measured absorbance area ratio.

4. Measurements in a Coal-Fired Power Plant

Testing was performed at the TVA Kingston plant in Harriman, TN, as a preliminary study on the feasibility of using the LTS-100 to measure gas temperatures in a full-scale coal-fired power plant setting. These tests were performed on Unit 9 of the Kingston plant. Figure 6 shows a sketch of the facility. This 200 MW unit is of a split furnace design and consists of two separate furnaces. One furnace is designated the superheat and the other is the reheat. The LTS-100 was installed on the reheat furnace of Unit 9. The furnace has a cross section of 23 ft x 25 ft, and is 95 feet from top to bottom.

Measurements were conducted in the radiant section of the furnace, above the fireball, as depicted in the sketch of Figure 6. The laser was passed through the combustion chamber along a 23-ft path, brought into and out of the boiler through open ports that were about 3.5 ft from the side wall and 56 ft above ground level. The probe hardware consisted of a collimator mounted on a tripod to launch the laser beam through an open port, and a detector mounted on another tripod to measure the transmission after passing through the furnace and out another open port. A fiber carried the laser light to the collimator, and a

coaxial cable carried the electrical signals from the detector to the LTS-100 processing unit.

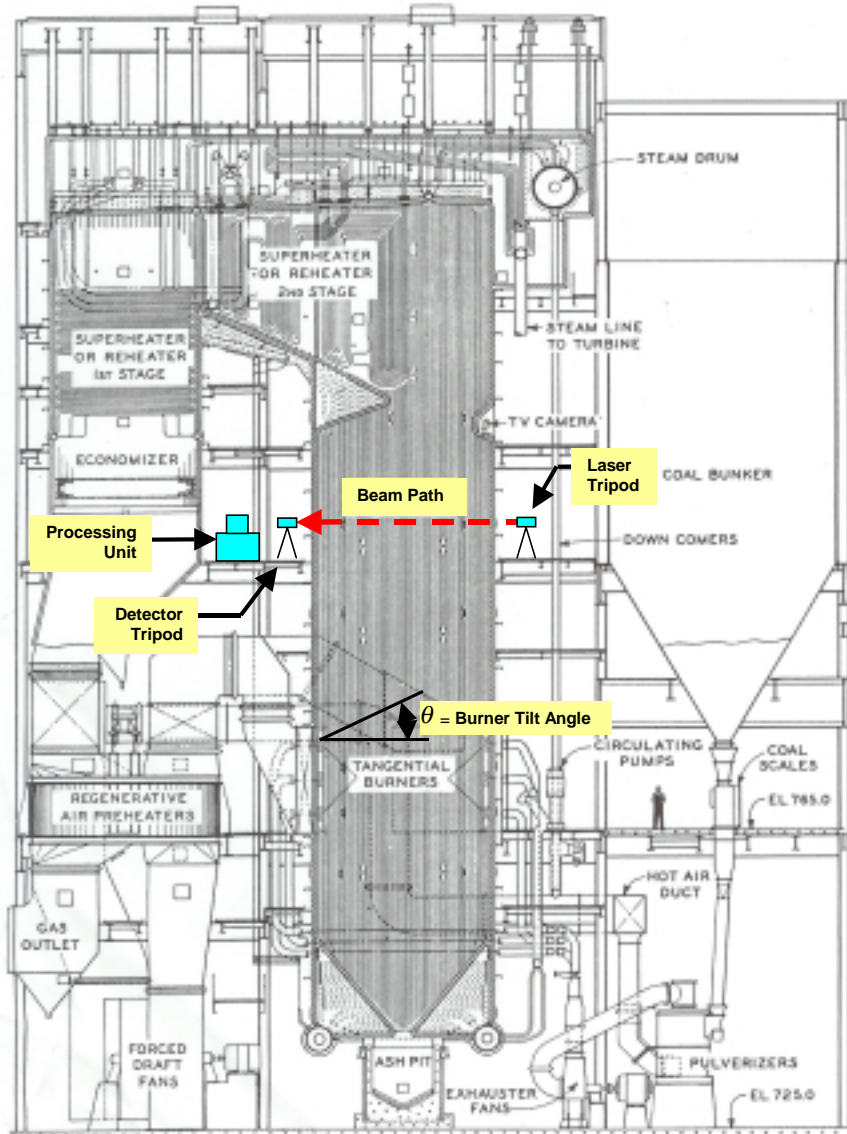


Figure 6. Side view of the experimental setup during in situ temperature measurements on Unit 9 of the TVA Kingston plant.¹²

System setup was performed while the power plant was in operation. Rough beam alignment was accomplished using a separate laser at a visible wavelength that was mounted adjacent to the collimator, parallel with the infrared (IR) beam. The visible beam was steered onto a target sheet located below the detector by adjusting the position of the tripod mount. Final alignment of the IR beam to the detector was performed to maximize the signal strength through fine adjustments to the pan and tilt angles of the IR beam collimator.

The LTS-100 detector consists of an InGaAs photodiode detector coupled to a lens and a 10-nm bandwidth filter to block luminous emission from the flame. Even with the filter

in place, significant luminosity was detected. However, phase sensitive detection of the modulated laser signal enabled the luminous emission to be subtracted from the raw signal, thus significantly eliminating the problem for this application. The raw data was digitized using a 5-MHz 12-bit digitizing board (National Instruments PCI-6110) in an expansion chassis with a laptop computer. Scans were taken at a rate of about 70 Hz, and temperatures were calculated from them and displayed in real time in a strip chart display.

Figure 7 shows a screen shot of the front panel during data collection. On the left are three plots. The top plot shows the raw signal and the middle plot shows the calculated absorbance, both displayed as functions of time during one 50- μ s scan. The bottom plot shows a real-time strip chart display of the temperature, calculated from the absorbance area ratio. Through a software selectable control, temperature is displayed as either an instantaneous measurement, or a running average of a user-specified number of consecutive measurements. Temperature time history and individual absorbance spectra can be written to file by selecting a software switch. In all of the measurements reported here, the data were stored to file as a running average of 10 points, corresponding to a measurement bandwidth of roughly 7 Hz.

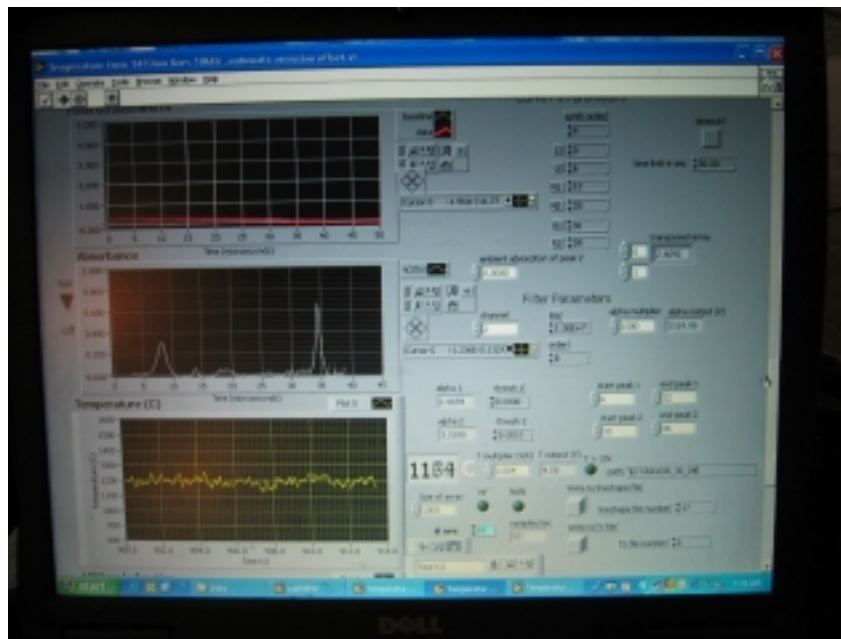


Figure 7. Screen shot of the LTS100 software during operation at the TVA Kingston coal-fired powerplant.

5. Results

A 10-kHz triangle wave was used to drive the laser, with only downward sloping parts of the cycle being used for data analysis. Figure 8 shows a typical absorption trace from a single scan of the laser for which the measured temperature was about 2250 °F. This time trace looks quite similar to the simulated spectrum of Figure 1, except that absorption line on the left is somewhat wider than the one on the right, while in the simulation they are of similar width. This may be caused, for example, by the broadening coefficients from HITRAN being inaccurate, or by the scanning rate of the laser being nonlinear. In either

case, these effects would be accounted for in the calibration of the sensor, and therefore should not affect the accuracy of the temperature measurements.

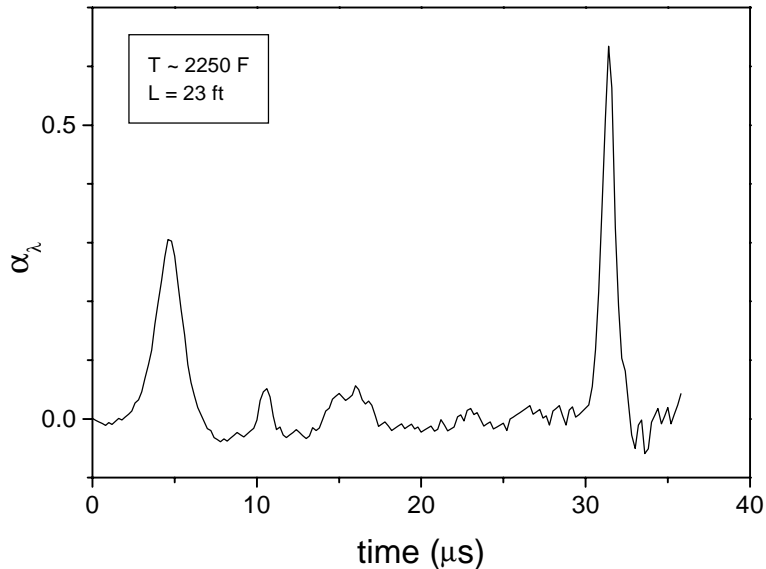


Figure 8. A typical H₂O absorption scan measured *in situ* at the TVA Kingston plant over a 23-ft path.

The minimum detectable absorbance was found in off-line measurements to be about 1×10^{-3} , limited by etalon noise. The absorbance levels over the pathlength of 23 ft were on the order of 5×10^{-1} , resulting in a theoretical signal to noise ratio of about 500. However, when making measurements through the flame zone, the raw signal levels are significantly less due to attenuation of the beam by soot. The effect of this attenuation is to decrease the dynamic range of the digitizing board, causing the minimum detectable absorbance to increase to about 1×10^{-2} , limited by bit noise. However, even at these high absorbance levels, the signal to noise ratio of the absorbance measurement is still a respectable 50.

Signal processing works as follows. A synchronous output from the function generator triggers the data acquisition for each scan, digitizing about 250 data points. The absorbance areas are computed by summing the data points that make up each absorption line, and the ratio of areas is computed. Next, the temperature is computed from the area ratio using the calibration curve of Figure 5. This results in a new temperature value about every 14 ms, since it takes about this long for the processing using the current system. As computer speeds increase, the update rate will increase, perhaps up to the limit imposed by the scanning rate of the laser, which is about 10 kHz.

Figure 9 shows a time history of temperature during a period of about 18 minutes (1100 s) while the burner tilt angles were being varied. The dark blue line shows data from a running average of 10 points, resulting in 140 ms averages, while the pink line shows data that has been low-pass filtered, having an effective averaging time of about 1 minute. Gaps appearing in the data, corresponding to times during which the data collection program was stopped to save the data to disk. At time $t = 0$, the burner tilt angle was changed from $+4^\circ$ to -20° . Figure 6 shows how this angle is defined. After the change, the temperature can be seen to drop at first, and then come back up to its original level after about two minutes. At $t = 120$ s, the tilt angle was changed to $+20^\circ$, after

which a sharp decrease in temperature is seen to occur. At $t = 360$ s the tilt angle is changed again back to -20° , apparently causing a sharp decrease in temperature again, followed by a gradual increase. Finally, at $t = 600$ s, control of the burner tilt angles was returned to the unit operator. From this point onward, burner tilt angle was governed by the unit's steam temperature control system.

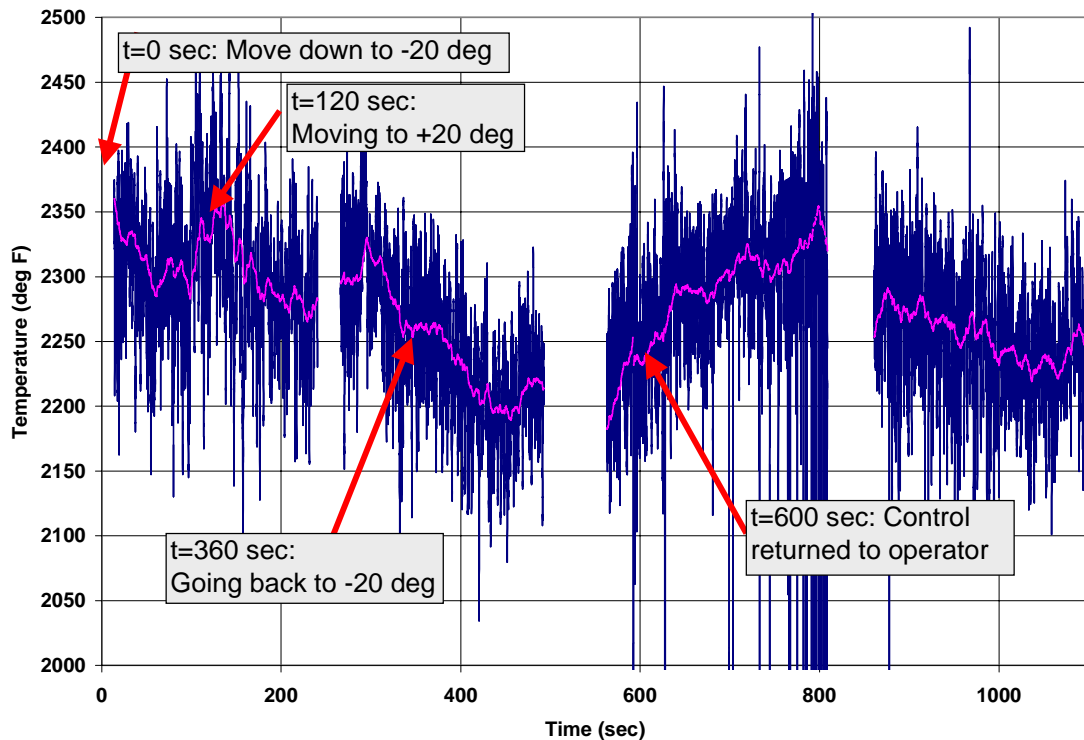


Figure 9. Time history of temperature from the line area ratio from *in situ* measurements at the TVA Kingston coal fired power plant during various positions of the burner tilt angle.

Figure 9 shows that the magnitudes of the temperatures recorded were between 2200°F and 2350°F . These are in reasonable agreement with temperatures measured by Teichert et al.⁶ using a pyrometer in another coal fired power plant, which were around 2130°F . As Figure 9 shows, at each change in burner tilt angle, a change in the measured temperature was observed. However, the value of temperature was not always the same for a given tilt angle, perhaps due to transient heating effects. These results suggest that the LTS-100 sensor can be used to actively monitor the temperature *in situ* in the flame zone to optimize burner control settings, perhaps to improve efficiency or to reduce slagging.

6. Conclusions

A commercially available diode laser temperature sensor, the MetroLaser LTS-100, has been successfully demonstrated in a full-scale coal-fired power plant. Temperature is obtained from the absorption line area ratio from a $50\text{-}\mu\text{s}$ scan of a diode laser. The sensor enables *in situ* measurements at data rates up to 70 Hz that may be used for process control or monitoring combustor health. Results are presented here showing changes in flame temperature that correspond to the burner tilt angle, suggesting, for

example, that the sensor could help an operator to find optimum conditions. These results show that the LTS-100 has the capability to provide accurate real time temperature measurements in a flame zone for monitoring and control in an industrial setting.

Acknowledgements

The EPRI I&C Center is thanked for contributing to this testing through the very capable support of the Center's staff. The TVA Kingston Steam Plant management is thanked for permitting testing of the MetroLaser LTS-100 in their facility. The Plant's personnel, in particular the control room staff for Units 1, 5 and 9, are thanked for their cooperation. Clyde W. Besley of the TVA Fossil Power Group and Robert L. Frank of the EPRI I&C Center coordinated the burner tilt angle testing on Unit 9.

This research was supported, in whole or in part, by DOE Grant No. DE-FG03-99ER82828 and such support does not constitute an endorsement by DOE of the views expressed in this article.

REFERENCES

- ¹ R. K. Hanson and P. K. Falcone, "Temperature Measurement Technique for High Temperature Gases Using a Tunable Diode Laser", *Applied Optics* **17**, pp.2477-2480 (1978).
- ² J. Ried, J. Shewchun, B. K. Garside, and E. A. Balik, "High Sensitivity Pollution Detection Employing Tunable Diode Lasers", *Applied Optics* **17**, pp. 1185-1190 (1978).
- ³ T. P. Jenkins, P. A. DeBarber, and M. Oljaca, "A Rugged Low-Cost Diode Laser Sensor for H₂O and Temperature Applied to a Spray Flame", AIAA 2003-0585, 41st AIAA Aerospace Sciences Meeting and Exhibit, Reno, NV (2003).
- ⁴ T. P. Jenkins, P. A. DeBarber, and M. Oljaca, "Diode Laser Sensor for H₂O and Temperature Applied to Measurements in an Industrial Combustion Vapor Deposition Torch", Proceedings of the Third Joint Meeting of the U.S. Sections of The Combustion Institute, Chicago, IL (2003).
- ⁵ P.A. DeBarber, T.P. Jenkins, E.H. Scott, "Multiple Channel Tunable Diode Laser Sensors for Industrial Combustion Monitoring," 2001 Joint International Combustion Symposium, Kauai, HI (2001).
- ⁶ H. Teichert, T. Fernholz, and V. Ebert, "Simultaneous In Situ Measurement of CO, H₂O, and Gas Temperatures in a Full-Sized Coal-Fired Power Plant by Near-Infrared Diode Lasers", *Applied Optics* **42**, pp.2043-2051 (2003).
- ⁷ T. P. Jenkins, P. A. DeBarber, E. H. Scott, V. G. McDonell, and T. N. DeMayo, "A Rugged, Low-Cost Diode Laser Sensor For H₂O And Temperature", Western States Section/The Combustion Institute Spring Meeting, San Diego, CA (2002).
- ⁸ T. P. Jenkins, P. A. DeBarber, J. Shen, and V. G. McDonell, "A Simple, Rugged Diode Laser Sensor for Temperature Applied to Measurements in a Low NO_x Burner",

American Flame Research Committee International Symposium on Combustion Research and Industrial Practice, Livermore, CA (2003).

- ⁹ E.R. Furlong, R.M. Mihalcea, M.E. Webber, D.S. Baer, and R.K. Hanson, “Diode-laser sensor system for closed-loop control of a 50-kW incinerator,” 33rd Joint Propulsion Conference. AIAA-97-2833 (AIAA, NY 1997).
- ¹⁰ M.P. Arroyo and R. K. Hanson, “Absorption Measurements of Water-Vapor Concentration, Temperature, and Line-Shape Parameters Using a Tunable InGaAsP Diode Laser”, *Applied Optics* **32**, pp.6104-6116 (1993).
- ¹¹ L.S. Rothman, C. P. Rinsland, A. Goldman, S. T. Massie, D. P. Edwards, et al., “The HITRAN Molecular Spectroscopic Database and HAWKS (HITRAN Atmospheric Workstation): 1996 Edition”, *Journal of Quantitative Spectroscopy and Radiation Heat Transfer* **60**, pp.665-710 (1998).
- ¹² “The Kingston Steam Plant Technical Report No. 34”, Tennessee Valley Authority, Knoxville, Tennessee 1965.